J. theor. Biol. (2001) **208,** 329–343
doi:10.1006/jtbi.2000.2222, available online at http://www.idealibrary.com on IDEAL®

Variability of Excitatory Currents due to Single-Channel Noise, Receptor Number and Morphological Heterogeneity

J. Trommershäuser*†, S. Titz‡, B. U. Keller‡ and A. Zippelius*

**Institut für Theoretische Physik, Universität Göttingen, Bunsenstr. 9, and ‡Zentrum Physiologie und Pathophysiologie, Universität Göttingen, Humboldtallee 23, D-37073 Göttingen, Germany*

(*Received on* 9 *November* 1999, *Accepted on* 20 *October* 2000)

Patch clamp recordings of excitatory postsynaptic currents (EPSCs) in central neurons reveal large fluctuations in amplitudes and decay times of AMPA-receptor-mediated EPSCs. By using Monte Carlo simulations of synaptic transmission in brainstem interneurons, we tested several hypothesis that could account for the observed variability. The coefficient of variation (CV) of 0.5 for miniature amplitudes cannot be explained by fluctuations in vesicle content or receptor distribution, but is traced to variations in receptor number, which is estimated as 77 ± 39 receptors per bouton. As the variability of rise times reflects fluctuations in size of the post-synaptic density and heterogeneity of the receptor distribution, the relatively small $CV = 0.37$ of experimentally determined values points to a homogeneous arrangement of receptors. Within our model the large variability of decay times ($CV = 0.49$) can only be explained by fluctuations in the transmitter time course (mean residence times of 0.4 ± 0.13 ms), presumably resulting from heterogeneities in synaptic morphology. Hence, our simulations indicate that different noise sources control the variability of amplitudes, rise and decay times. In particular, the distribution of decay times yields information about the synaptic transmission process, which cannot be obtained from other observables.

1. Introduction

Many aspects of central synaptic function are not yet understood in detail, including the basic mechanisms of synaptic transmission. One important line of investigation includes the study of so-called miniature synaptic currents—post-synaptic responses which result from the spontaneous release of single neurotransmitter-containing vesicles (e.g. Bekkers *et al.*, 1990; Bekkers & Stevens, 1995; Borst *et al.*, 1994; Edwards *et al.*, 1990; Glavinovic, 1999; Frerking *et al.*, 1995; Liu *et al.*, 1999; Nusser *et al.*, 1997; Tang *et al.*, 1994). Experiments generally yield a wide range of variability of these quantal responses. Learning about possible sources of this variability is essential in understanding synaptic function. The large quantal variability has predominantly been observed in the miniature amplitude distribution of post-synaptic currents (see Liu *et al.*, 1999, Nusser *et al.*, 1997 for further references) and its origin has been discussed controversially since. It has been suggested that variations in mEPSC amplitudes arise from presynaptic mechanisms such as transmitter release (Bekkers *et al.*, 1990; Glavinovic, 1999; Forti *et al.*, 1997; Frerking *et al.*, 1995; Liu *et al.*, 1999) or that they are caused by fluctuations located on the post-synaptic side as, for instance, variations in the receptor number (Borst *et al.*, 1994;

†Author to whom correspondence should be addressed.
E-mail: trommer@theorie.physik.uni-goettingen.de

0022–5193/01/030329 + 15 $35.00/0

Edwards *et al.*, 1990; Nusser *et al.*, 1997; Tang *et al.*, 1994). Closely related to this discussion is the question whether synapses are saturated after the release of a single vesicle. It is commonly believed that at central synapses an abundance of neurotransmitter hits a very limited number of postsynaptic receptors [see Edwards (1995) and Walmsley *et al.* (1998) for reviews]. Still agreement regarding the question of saturation of postsynaptic receptors is lacking. Experimental and theoretical approaches have been chosen to address this question and have led to the conclusion that the release of a single vesicle of glutamate activates most of non-NMDA receptors, i.e. causes an open probability $\geqslant 70\%$ (Jonas *et al.*, 1993; Kleinle *et al.*, 1996; Kullmann *et al.*, 1999; Min *et al.*, 1998; Silver *et al.*, 1996; Spruston *et al.*, 1995; Tang *et al.*, 1994; Wahl *et al.*, 1996). But also open probabilities of less than 50% have been observed in mEPSCs (Liu *et al.*, 1999; Mainen *et al.*, 1999; Silver *et al.*, 1996), often coming along with large fluctuations in mEPSC amplitudes, which then are thought to be due to fluctuations in vesicle content (Harris & Sultan, 1995; Liu *et al.*, 1999) or point of release (Uteshev & Pennefather, 1996). These contradicting results are brought together in the idea that receptor occupancy might be sensitive to several factors, such as synaptic morphology, the anatomy of the synaptic cleft, the time course of transmitter clearance, and that these properties most probably vary from one synapse to the next (Clements, 1996; Edwards, 1995; Frerking & Wilson, 1996; Harris & Kater, 1994; Lim *et al.*, 1999; Liu & Tsien, 1995; Min *et al.*, 1998; Oleskevich *et al.*, 1999; Rossi *et al.*, 1995; Silver *et al.*, 1996; Walmsley *et al.*, 1998).

In this paper, we address the question of origins of synaptic variability from a novel point of view by not only studying mechanisms that shape the distribution of amplitudes, but also those of *rise and decay times*. Decay times of AMPA-mediated mEPSCs are slower than the fast deactivation of AMPA channels (Edmonds *et al.*, 1995; Hausser & Roth, 1997; Spruston *et al.*, 1995), so that desensitization contributes to shaping the time course of post-synaptic currents (Glavinovic, 1999; Hausser & Roth, 1997; Jonas *et al.*, 1993; Jones & Westbrook, 1996; Spruston *et al.*, 1995; Wahl *et al.*, 1996). This is in accordance with measurements, which indicate that glutamate remains in the synaptic cleft for almost a millisecond (Clements *et al.*, 1992; Clements, 1996). We therefore expect that decay times of mEPSCs can provide additional information about the time course of glutamate in the cleft. A similar line of reasoning has been pursued in several experiments and simulations (Barbour *et al.*, 1994; Diamond & Jahr, 1997; Holmes, 1995; Tong & Jahr, 1994), where it was shown that changes in the time course of glutamate lead to alterations in EPSC decay times.

Our patch-clamp recordings on brainstem interneurons in the nucleus tractus solitarius (NTS) (Titz & Keller, 1996, 1997) show that a glutamate concentration of 1 mM, which corresponds to the transmitter concentration released from a single vesicle (Clements, 1996; Edwards, 1995), activates $\sim 72\%$ of non-NMDA receptors. Based on this, we assume that the population of post-synaptic receptors is mostly saturated by the release of a single vesicle, leaving little room for synaptic variability caused by pre-synaptic parameters such as fluctuations in release probability or vesicle content. Instead the variations in mEPSCs amplitudes are thought to reflect differences in receptor number between synaptic boutons as well as the intrinsic noise of the receptor dynamics (Faber *et al.*, 1992; Tang *et al.*, 1994; Trommershäuser *et al.*, 1999). Another source of variability may arise from inhomogeneities in receptor density (Wahl *et al.*, 1996) or different receptor arrangements due to variable sizes of the post-synaptic density (PSD) (Edwards, 1995; Lim *et al.*, 1999; Oleskevich *et al.*, 1999), although our recent theoretical studies have pointed out that the contribution of spatial fluctuations to the variability of mEPSCs is small (Trommershäuser *et al.*, 1999).

In the following, we will utilize Monte Carlo simulations of mEPSCs to test the effect of synaptic parameters such as receptor number, synaptic morphology and transmitter dynamics on the distribution of amplitudes, rise and decay times of non-NMDA-mediated mEPSCs of brainstem interneurons. We will demonstrate that fluctuations in miniature amplitudes are resolved by variations in the synaptic receptor number. In contrast, the variability of EPSC decay times proves to be independent of fluctuating receptor numbers, and is explained in the

frame of our model only by a heterogeneity in synaptic morphology affecting the transmitter motion. This effect of the synaptic morphology does not occur in any other observable, suggesting that the analysis of the distribution of decay times yields additional insight into synaptic function.

2. Experimental Procedure

Transverse slices of the brainstem from 10 to 14-day-old rats containing the parvocellular and medial nuclei of the NTS were prepared as previously described (Titz & Keller, 1997). Slices were kept at room temperature in continuously bubbled (95% O_2, 5% CO_2) extracellular solution (118 mM NaCl, 3 mM KCl, 1 mM $MgCl_2$, 25 mM $NaHCO_3$, 1 mM NaH_2PO_4, 1.5 mM $CaCl_2$, 10 mM glucose) at pH 7.4 until transferred to the recording chamber. Whole-cell recording experiments (Hamill *et al.*, 1981) were started after at least 1 hr of incubation to improve recovery. During experiments, slices were continuously superfused with the solution described above (3.2 ml min^{-1}) at room temperature ($22 \pm 2°C$). All perfusing solutions contained 10 μM bicuculline (Sigma, Germany) to block $GABA_A$-receptor-mediated inhibitory post-synaptic currents. For recording of miniature EPSCs, 1 μM tetradotoxin (TTX, SIGMA) was added to the perfusing solution. In some experiments, 100 mM sucrose was added to increase the frequency of miniature EPSCs. In experiments with low Ca^{2+}/Mg^{2+} ratio the Ca^{2+} concentration was varied between 1.5 and 0.7 mM and the Mg^{2+} concentration was changed accordingly to maintain a constant divalent ion concentration (Titz & Keller, 1996, 1997).

Patch pipettes used for single-electrode voltage-clamp recordings were pulled from borosilicate glass tubing (Kimble, USA) and heat-polished before use. When filled with intracellular solution (in mM: 140 CsCl, 10 HEPES, 10 EGTA, 1 $CaCl_2$, 2 $MgCl_2$, 4Na_2-ATP, 0.4 Na_3-GTP, 4.5 mg ml^{-1} Neurobiotin, adjusted to pH 7.3 with CsOH), they had a resistance of 1.8–2.5 MΩ. Currents were amplified using an EPC-9 (HEKA Elektronik Lambrecht, Germany) amplifier. Whole-cell currents were recorded with sampling frequencies of 5 kHz, filtered (3-pole-Bessel filter 10 kHz, 4-pole Bessel filter 2.9 kHz) and stored on the hard disk of a Macintosh computer for off-line analysis with programs Pulse fit (HEKA Elektronik, Lambrecht, Germany) and Igor (Wavemetrics, Lake Oswego, OR, USA). For recordings from outside-out patches the sampling frequency was increased to 10 kHz. Optimal series resistance compensation was employed as previously described (Llano *et al.*, 1991) obtaining the values of *Rs* and *Cm* from the settings of the capacitance cancellation circuitry of the patch-clamp amplifier. Typical series resistance ranged from 8 to 15 MΩ. Cells with series resistances higher than 15 MΩ were not included in the analysis. An optimal series resistance compensation was performed by using the series resistance compensation circuitry of the EPC-9 patch clamp amplifier according to Hamill *et al.* (1981). The membrane potential of the recorded cell was held at − 60 mV. No compensation was made for the liquid junction potential. Values of *Rs* and *Cm* were regularly monitored during an experiment. EPSCs were evoked in pNTS neurons by electrical stimulation (isolated stimulator, HI-Med, H15) of afferent fibers in the ipsilateral parvocellular or medial NTS using a standard patch pipette (2–3 MΩ) filled with intracellular solution. To favor single-fiber stimulation stimulus intensity was set to a minimum (8–30 V). Stimulation pulses lasting 200 μs were delivered at a frequency of 0.3 Hz. Outside-out patches excised from NTS cells were exposed to agonist containing solution (1 mM glutamate in extracellular solution) using a high-voltage piezoelectric crystal (Physik Instrumente, Waldbronn, Germany) to rapidly move an application pipette (Barbour *et al.*, 1994; Franke *et al.*, 1987; Titz & Keller, 1997). The flow of solutions from the pipette and from the bath (3 ml min^{-1}) were arranged to be parallel to favor laminar flow of the agonist containing solution.

2.1. ANALYSIS

Kinetic analysis was performed on individual EPSCs. The rise time was measured as the time to rise from 20 to 80% of the EPSC peak amplitude. For determining the decay time constant, a single exponential was fitted from peak to baseline. The peak amplitude was calculated as the difference

between the mean current before the EPSC and the peak amplitude. Latencies were defined as the time from the end of the stimulus to the beginning of the EPSC as determined by the crossing point between the baseline and a back-extrapolated line connecting the curve points at 20 and 80% of the amplitude. Numerical values are given throughout the text as mean $\pm$ standard deviation. Averages of EPSC kinetics were calculated by taking the mean value for all EPSCs measured. To further illustrate the statistical basis of measurements, we also indicated the number of cells investigated. When the total number of EPSCs is not explicitly stated, averages were calculated for each cell and the indicated SD reflects variations between cells.

The contribution of background noise on the variability of EPSC kinetics was investigated in detail by simulation of elementary synaptic responses. In this case, EPSCs in pNTS interneurons were simulated with an average amplitude of 15 ± 3 pA, mean monoexponential decay time constants of 2.9 ms and a sampling interval of 5 kHz. A Gaussian background noise was added with a mean amplitude of 1.5 pA. Decay kinetics of simulated EPSCs were then approximated by our mono-exponential fitting algorithm. The distribution of decay time constants of 1000 simulated EPSCs was well approximated by a Gaussian function with a mean value of 2.9 ms and a standard deviation of 0.3 ms, indicating that a variation of this magnitude resulted from background noise. Similar results were obtained for rise times and amplitudes, indicating that variations due to background noise accounted for a CV of 0.1 in the kinetic parameters.

2.2. NON-STATIONARY FLUCTUATION ANALYSIS

The maximum open probability of non-NMDA receptors in outside-out patches exposed to 1 mM of glutamate is estimated using the method of non-stationary fluctuation analysis (see e.g. Hille, 1992). The average current $I(t)$ is calculated averaging ten individual current responses from nucleated outside-out patches (Titz & Keller, 1997). To obtain the time-dependent variance $\sigma(I(t))^2$ every individual response is subtracted from the averaged current and the difference is squared. The 119 data points for $\sigma(I(t))^2$ are fitted by

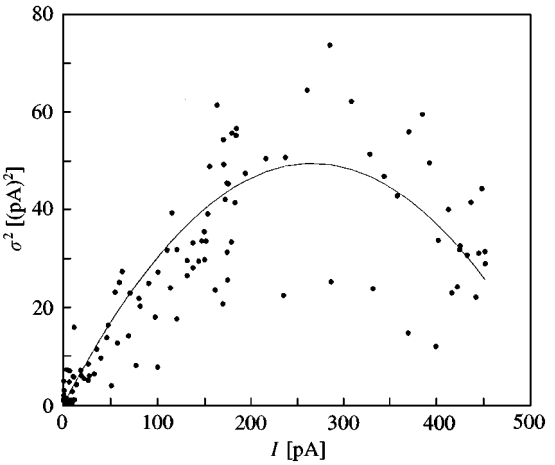

FIG. 1. Mean variance for a total of ten responses obtained in outside-out patches as a function of the mean current for all ten responses. The data are fitted with eqn (1) (see Section 2) to determine N and $P_{o,max}$.

$$\sigma^2 = iI - \frac{1}{N} I^2, \tag{1}$$

(Sigworth, 1980) for a singe-channel current i of 0.372 pA (Titz & Keller, 1997).

The fit yields (Fig. 1) an average number of 1431 ± 24 receptors (68.3% confidence interval) in the outside-out patch. This corresponds to a maximum open probability of 72% at peak amplitudes of 420 pA (Fig. 1).

3. Theory

3.1. KINETIC MODEL OF AMPA RECEPTOR

The AMPA receptor is modeled using the kinetic three-state model defined by eqn (2), which has been shown to account for the basic features of the synaptic transmission process (Destexhe *et al.*, 1994; Marienhagen *et al.*, 1997):

$$\mathrm{D} \underset{\bar{k}_d}{\overset{k_r}{\rightleftarrows}} \mathrm{R} \underset{k_c}{\overset{\bar{k}_o}{\rightleftarrows}} \mathrm{O}. \tag{2}$$

Here R denotes the closed unbound, O the open conducting and D the desensitized state. The transition rates between the open state O and desensitized state are usually small (Jonas *et al.*,

TABLE 1
Kinetics of AMPA receptors as estimated from rapid application of glutamate to outside-out patches in interneurons (*Titz & Keller*, 1997)

Desensitization time constant: τ_{des} (1 mM) = 5.47 ± 1.3 ms
Deactivation time constant: τ_{dea} = 0.8 ± 0.3 ms
Resensitization time: τ_{res} = 50 ± 12 ms
Maximum open probability: $P_{O,max}$ ([1 mM]) = 72%

1993; Hausser & Roth, 1997) and are neglected in this context for the sake of simplicity. To undergo a transition into the open or desensitized state the receptor has to bind two glutamate molecules (see e.g. Edmonds *et al*., 1995), which is reflected by the transmitter dependency of the transition rates $\tilde{k}_o$ and $\tilde{k}_d$. In a first approximation, the two binding steps of glutamate (Jahn *et al*., 1998) are assumed to be rapid compared to the time-scales of channel opening and desensitizing (Hausser & Roth, 1997; Jahn *et al*., 1998, 1993; Spruston *et al*., 1995) so that the concentration dependency of $\tilde{k}_o$ ($\tilde{k}_d$, respectively) is given by

$$\tilde{k}_o = k_o[\mathrm{Glu}]^2/([\mathrm{Glu}] + K_B)^2, \qquad (3)$$

with K_B denoting the equilibrium constant (see e.g. Colquhoun & Hawkes, 1995). The kinetic parameters of the reaction scheme (2) are estimated by calculating the open probability $P_O(t)$ as described in Marienhagen *et al*. (1997). The analytical solutions for $P_{O,max}([\mathrm{Glu}])$, $\tau_{des}([\mathrm{Glu}])$, τ_{dea} and τ_{res} are then fitted to the outcome of experiments on outside-out patches of brainstem interneurons (Titz & Keller, 1997), which are displayed in Table 1.

This yields the kinetic rate constants in Table 2 which subsequently are used in the Monte Carlo simulations to model the AMPA receptor.*

3.2. MONTE CARLO SIMULATIONS OF EPSCs

In the Monte Carlo simulation we model a single synaptic bouton as a two-dimensional disc, which is bounded by an absorbing boundary at the radius r_{abs} (Fig. 2). The model, its underlying assumptions and range of validity has been discussed in detail elsewhere (Trommershäuser *et al*., 1999). In particular, it has been shown that the neurotransmitter rapidly equilibrates across the synaptic cleft within a few microseconds, which justifies our two-dimensional model of the cleft. The absorbing boundary comprises the effects of transporters on the transmitter dynamics and glutamate uptake by extra-synaptic mechanisms (Trommershäuser *et al*., 1999). The post-synaptic receptors (total number: n_{rec}) are homogeneously randomly distributed within the post-synaptic density (PSD) of radius r_{PSD} ($r_{PSD} < r_{abs}$). It is assumed that the content of a single vesicle N_T is released instantaneously from a single point $\mathbf{r}_0 = (x_{release}, y_{release})$, which is chosen randomly within the PSD. The transmitter molecules spread within the synaptic cleft with an effective diffusion constant D_{net} according to Fick's law before being irreversibly taken out of the simulation after having crossed the absorbing boundary at radius r_{abs}.

Information about the synaptic geometry and the number of transmitter molecules released is taken from Edwards (1995) and Bruns & Jahr

*Outside-out patch-recordings of NTS neurons yield a single time constant for deactivation and desensitization and indicate a kinetically homogeneous AMPA receptor population in NTS neurons (Titz & Keller, 1997).

TABLE 2
Kinetic rate constants for the AMPA receptor

k_0	k_d	k_c	k_r	K_B
6 ms^{-1}	1.1 ms^{-1}	1.25 ms^{-1}	0.02 ms^{-1}	450 μM

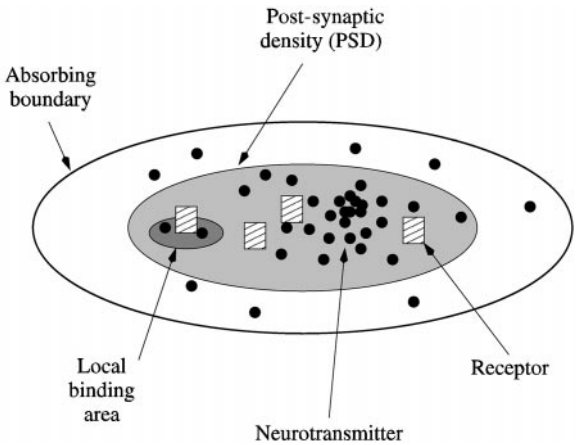

FIG. 2. Monte Carlo simulations: model of a single synaptic bouton.

(1995). The distribution of rise times is used to yield an estimate of the effective diffusion constant $D_{net} = 40\ \mathrm{nm}^2\,\mu\mathrm{s}^{-1}$, which is in accordance with the range given by Kleinle *et al.* (1996), Bennett *et al.* (1997), Agmon & Edelstein (1997), and Trommershäuser *et al.* (1999).

In the Monte Carlo simulation of a single synaptic bouton, the concentration profile and the states of all receptors are updated simultaneously. For each discrete time step Δt a "new" distribution of transmitter molecules is generated, a possible change in the states of all receptors is calculated and the number of open channels is computed at every time step [see Trommershäuser *et al.* (1999) for details and further references].† This yields the number of open channels or the open probability, respectively, as a function of time. For a series of sweeps, which are run for a set of given synaptic parameters but varying initializations of the random number generator, distributions of amplitudes, rise and decay times are generated and compared with recordings of mEPSCs. The coefficient of variation (CV—standard deviation/mean) is taken as an index of variability.

3.3. CALCULATION OF THE RESIDENCE TIME OF TRANSMITTER IN THE CLEFT

The mean residence time of neurotransmitter in the cleft can be calculated for a given synaptic geometry, i.e. the absorbing boundary r_{abs} and extension of the PSD r_{PSD} and any point of release $\mathbf{r}_0 = (x_{release}, y_{release})$. As shown in Trommershäuser *et al.* (1999) the residence time $\langle T \rangle$ is then given by

$$\langle T \rangle = \frac{2 r_{PSD} r_{abs}}{D_{net}} \sum_{n=1}^{\infty} \frac{1}{\lambda_{0n}^3} \frac{J_0(\alpha_{0n} r_0)\, J_1(\alpha_{0n} r_{PSD})}{[J_1(\lambda_{0n})]^2},$$

$$r_0 = \sqrt{x_{release}^2 + y_{release}^2}, \quad \alpha_{0n} = \frac{\lambda_{0n}}{r_{abs}}.$$

†The choice of the simulation time step Δt depends on the time-scales involved. As discussed in Trommershäuser *et al.* (1999) we choose a time step of 4 μs to account for the microscopic change in the transmitter concentration which is considerably faster than the shortest transition time between two receptor states. It was shown in Trommershäuser *et al.* (1999) that larger and smaller time steps do not alter the results of the simulation.

Here J_m denotes the mth Bessel function of the first kind and λ_{mn} the n-th zero of J_m.

3.4. COMPUTATIONAL PROCEDURE

The computer simulations and numerical routines were written in the C language, compiled and run on Pentium PCs. Random numbers were generated using the ran2 routine (Press *et al.*, 1992).

4. Results

In central neurons patch clamp recordings of excitatory synaptic currents reveal substantial fluctuations in amplitudes and decay times of AMPA-receptor-mediated EPSCs. In our present study, we investigated in detail excitatory synaptic transmission in brainstem interneurons in the NTS from rat, mainly because their electrically compact shape permits high-resolution electrophysiological recordings of synaptic responses. Figure 3 illustrates EPSCs in NTS interneurons (from Titz & Keller, 1996) during repetitive stimulation of pre-synaptic afferents. Neurotransmitter release probability was minimized by reduced extracellular calcium concentration as previously described (Titz & Keller, 1996). The time course of mEPSCs exhibits large variations as displayed in Fig. 5. Miniature EPSCs yield distributions of maximum amplitudes (52.8 ± 26.4 channels open at peak amplitude, CV = 0.5), rise (0.30 ± 0.11 ms, CV = 0.37) and decay times (2.64 ± 1.30 ms, CV = 0.49) as

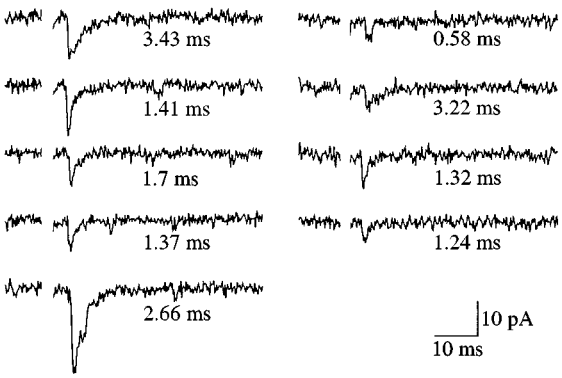

FIG. 3. Fluctuations in the time course of EPSCs recorded during single-fiber stimulation in the presence of low extracellular calcium concentration (0.8 mM) at a failure rate of 58% (taken from Titz & Keller, 1996).

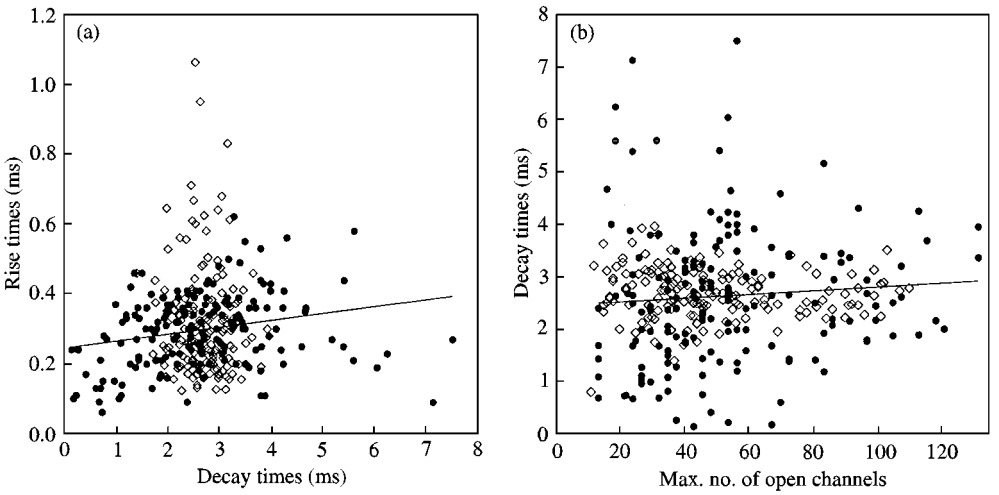

FIG. 4. Rise times as function of decay times (a) and decay times as function of maximum amplitudes (b) amplitude. Black circles indicate the results from recordings of mEPSCs, white diamonds the results from Monte Carlo simulations (see Fig. 5 for parameters); results from 169 recordings and simulation runs, respectively. The black line indicates the correlation of experimentally recorded rise and decay times (a: $r = 0.16$), and of decay times and amplitudes (b: $r = 0.07$).

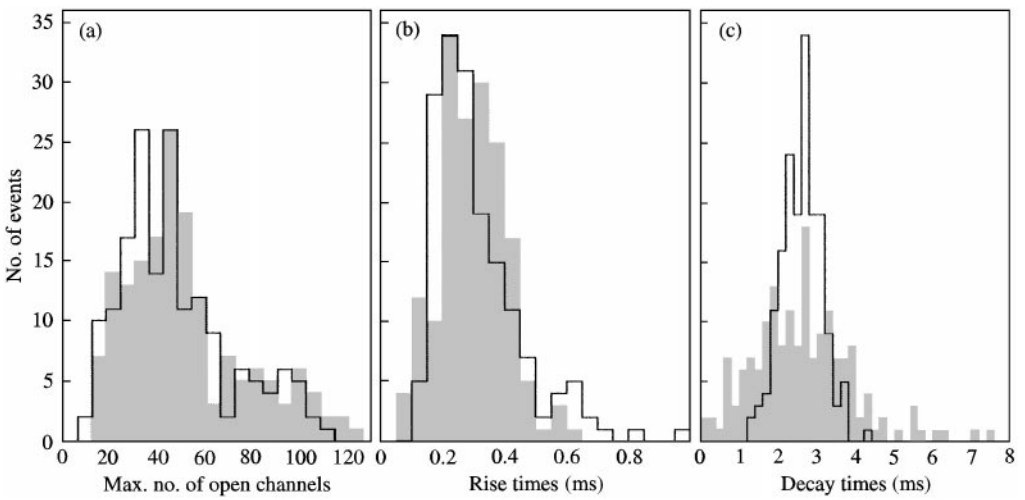

FIG. 5. Distributions of 169 mEPSC amplitudes (a), rise (b) and decay times (c) as recorded in low extracellular Ca^{2+} (gray columns) and as generated from Monte Carlo simulations (white columns). Simulations yielded a maximum of open channels of 47.8 $\pm$ 23.2 channels (experiments: 52.8 $\pm$ 26.4 channels), rise times of 0.32 $\pm$ 0.18 ms (experiments: 0.30 $\pm$ 0.11 ms) and decay times of 2.61 $\pm$ 0.48 ms (experiments: 2.64 $\pm$ 1.30 ms). Monte Carlo simulations were run for 4000 transmitter molecules released at each time randomly chosen release sites within the PSD of radius $r_{PSD} = 150$ nm; absorbing radius r_{abs} set to 500 nm.

displayed in Fig. 5. It should be noted here that the fluctuations of decay times (CV = 0.49) are larger than that reported for AMPA-mediated mEPSCs at CA3 and CA1 regions of rate hippocampus (Jonas *et al.*, 1993; CV = 0.22; Atassi & Glavinovic, 1999; CV = 0.34).

Variability in the mEPSC time course due to cable filtering is unlikely in these cells for the following reasons: First, NTS neurons are electrically compact as indicated by fast capacitive transients after membrane recharging (Titz & Keller, 1997). Second, rise times and decay times do not correlate significantly [Fig. 4(a)]. Such a correlation would be expected, because rising *and* decaying of an EPSC would be delayed for more distal synapses—provided the receptor

kinetics is the same for proximal and distal synapses. Outside-out patch recordings support the latter assumption (Titz & Keller, 1997). Third, rise times are relatively homogeneous, indicating that filtering effects are small. Hence we will not take dendritic filtering into account in our theoretical analysis. To identify the underlying sources of noise in the transmission process, we performed a detailed electrophysiological analysis of miniature EPSCs in NTS interneurons and compared the results with Monte Carlo simulations of synaptic transmission. Several mechanisms have been suggested as possible sources of synaptic variability and will be discussed in the following: Most likely miniature currents are recorded from various synaptic boutons, which might differ regarding *receptor number* (Borst *et al*., 1994; Edwards *et al*., 1990; Lim *et al*., 1999; Nusser *et al*., 1997; Oleskevich *et al*., 1999) and *receptor distribution* (Wahl *et al*., 1996), *vesicle content* (Liu *et al*., 1999) and *synaptic morphology* (Edwards, 1995; Walmsley *et al*., 1998). The latter, as well as heterogeneities in the transmitter-transporter interaction (Rusakov & Kullmann, 1998; Trommershäuser *et al*., 1999) have been suggested to affect the *transmitter dynamics in- and outside the cleft* (Kullmann *et al*., 1999). Furthermore, it has been pointed out (Bier *et al*., 1996; Faber *et al*., 1992, Trommershäuser *et al*., 1999) that in synaptic boutons with a small number of post-synaptic receptors, the *intrinsic noise of the receptor dynamics* provides the major contribution to synaptic variability.

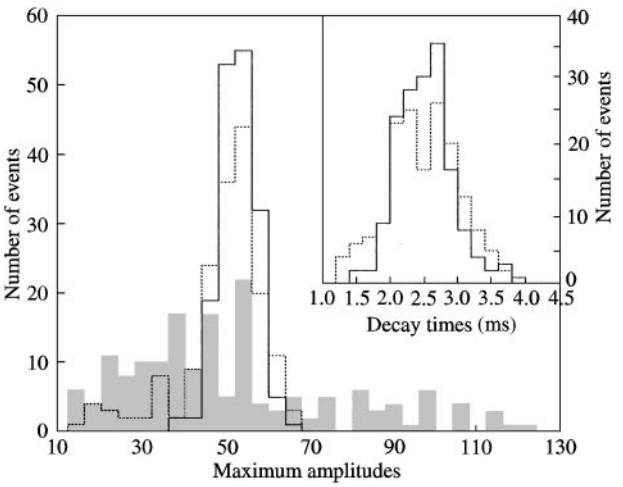

FIG. 6. Effect of fluctuations in vesicle content on amplitudes and decay times: distributions of maximum amplitudes and decay times (small inset) as generated from Monte Carlo simulations for a fixed number of 85 postsynaptic receptors and the release of 4000 transmitter molecules (white columns, ——: 53.1 ± 4.4 channels open at peak amplitude, decay times: 2.53 ± 0.42 ms) or a vesicle content, randomly chosen due to a Gaussian distribution with mean of 4000 molecules and a SD of 2000 molecules (white columns, ····, 49.5 ± 10 open channels; decay times: 2.5 ± 0.52 ms). Gray columns indicate the experimentally recorded miniature amplitudes.

4.1. THE BROAD DISTRIBUTION OF mEPSC AMPLITUDES IN BRAINSTEM INTERNEURONS IS DUE TO FLUCTUATIONS IN RECEPTOR NUMBER

In the simulations it has been assumed that a single mEPSC is caused by the release of, on average, 4000 glutamate molecules from a single vesicle at a randomly chosen release site located within a PSD of 300 nm diameter. The absorbing radius has been set to 500 nm. The chosen synaptic scenario implicates a residence time of glutamate in the cleft of $\langle T \rangle = 0.43 \pm 0.04$ ms.

First, Monte Carlo simulations have been performed to study the source of variation observed in the time course of miniature amplitudes. Monte Carlo simulations of a single synaptic bouton with a fixed number of 85 post-synaptic receptors yield a non-skewed distribution of amplitudes (53.1 ± 4.4 channels open at peak amplitude), which is too narrow to account for the range of experimentally observed fluctuations in the distribution of miniature amplitudes (52.8 ± 26.4 channels) as displayed in Fig. 6. The simulation results indicate that following the release of a single vesicle about $63 \pm 5\%$ of all channels open. Hence, as expected from the outcome of outside-out patch experiments (see above) the population of post-synaptic receptors is saturated to a large extent by the release of a single vesicle. Consistently, variations in vesicle content fail to cover the range of miniature amplitudes, if the number of post-synaptic receptors is fixed: As shown in Fig. 6 a strongly fluctuating vesicle content does not significantly increase the spectrum of miniature amplitudes. While vesicles containing < 1200 molecules yield smaller maximum amplitudes, the complementary effect for vesicles with a large amount of transmitter molecules does not occur due to the saturation of post-synaptic receptors. For the

same reason fluctuations in the transmitter dynamics as possibly caused by heterogeneities in synaptic morphology exhibit little effect on the amplitude distribution (see Fig. 8 for details). We conclude that variations in the miniature amplitude distribution of brainstem interneurons are not explained by variations in vesicle content, i.e. are not located on the pre-synaptic side, but are caused by fluctuations in post-synaptic receptor number.

The variation in maximum amplitudes is then due to the fact that the miniature amplitude distribution is caused by currents from *several* synaptic boutons containing a variable number of receptors.‡ We estimated receptor numbers by assuming that about 70% of post-synaptic receptors are activated by the release of a single vesicle (see Section 2). For every simulation run the number of post-synaptic receptors is calculated directly from our experimental data by dividing the recorded miniature amplitudes by the open probability 0.7 and the single-channel current of 0.372 pA (Titz & Keller, 1997). This yields a receptor number of 77 ± 39 post-synaptic receptors in a synapse (corresponding to 47.8 ± 23.2 channels open at peak amplitude) and allows to correctly cover the range of variation observed in experimental mEPSCs [Fig. 5(a)].

‡As indicated by the initial slope of σ^2 in Fig. 1 single-channel currents may fluctuate around the mean of $i = 0.372$ pA. The overall synaptic response, however, is gained by summing over single-channel current contributions. As confirmed by simulations (data not shown here) a number of approximately 85 receptors is sufficient to average out noise contributions to the amplitude CV due to fluctuations in the single-channel amplitude *i*: Simulations in which the single-channel amplitude is randomly altered according to a Gaussian distribution with a mean of 0.372 pA and CV of 0.4 (for a fixed number of 85 receptors, all other parameters chosen as for the white columns in Fig. 6) yield synaptic currents of 19.64 ± 1.76 pA (as compared to 19.75 ± 1.63 pA for constant *i*). We therefore consider contributions of fluctuating single channel currents to the observed variation in EPSC amplitudes to be negligible and use a constant single-channel current of $i = 0.372$ pA for our analysis. As outside-out patch-recordings of NTS neurons indicate kinetically homogeneous receptor populations in NTS neurons (Titz & Keller, 1997), we consider the possibility of strongly fluctuating mean EPSC amplitudes across different synapses (as possibly resulting from diverse previous synaptic activity) to be unlikely.

4.2. THE DISTRIBUTION OF RISE TIMES PROVIDES INFORMATION ABOUT THE RANGE OF POSSIBLE PSD SHAPES

For several types of central synapses a large variety of PSD shapes has been observed [see Edwards (1995) and Walmsley *et al.* (1998) for further references] and it has been suggested that variations in receptor distribution might contribute to synaptic variability of mEPSC amplitudes (Wahl *et al.*, 1996). If synaptic currents are expected to exhibit an effect due to the heterogeneity of receptor distributions it should mainly occur in the distribution of rise times because of the late activation of receptors at larger distances from the point of release. The results displayed in Fig. 7 support this conclusion: Doubling the radius of the PSD ($r_{PSD} = 300$ nm compared to $r_{PSD} = 150$ nm) broadens the distribution of rise times (Fig. 7). Such a broadening is beyond the experimentally observed width. We therefore conclude that fluctuations in PSD size are restricted to a range of approximately $r_{PSD} \sim 150$ nm. In other words, a heterogeneity of PSD shapes increases the range of variation of rise times which is not observed experimentally and hence not considered further in this work.

Furthermore, we find that the distribution of rise times is left unchanged for a fluctuating vesicle content (0.3 ± 0.14 ms, see also Fig. 6) or

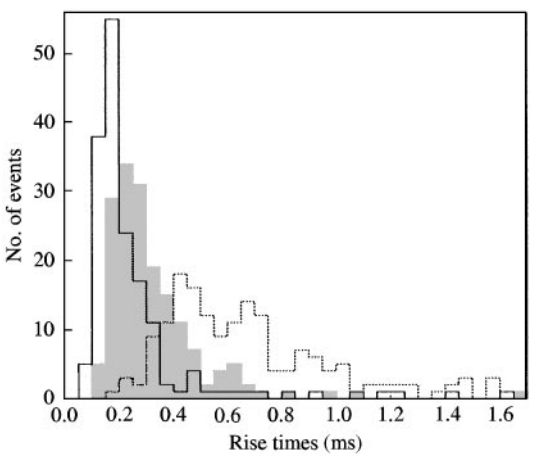

FIG. 7. Distribution of rise times for different extensions of the PSD; white columns/——: $r_{PSD} = 75$ nm, rise times: 0.25 ± 0.12 ms; gray columns: $r_{PSD} = 150$ nm, rise times: 0.32 ± 0.18 ms; white columns/·····: $r_{PSD} = 300$ nm, rise times: 0.70 ± 0.37 ms; rest of parameters as in Fig. 5.

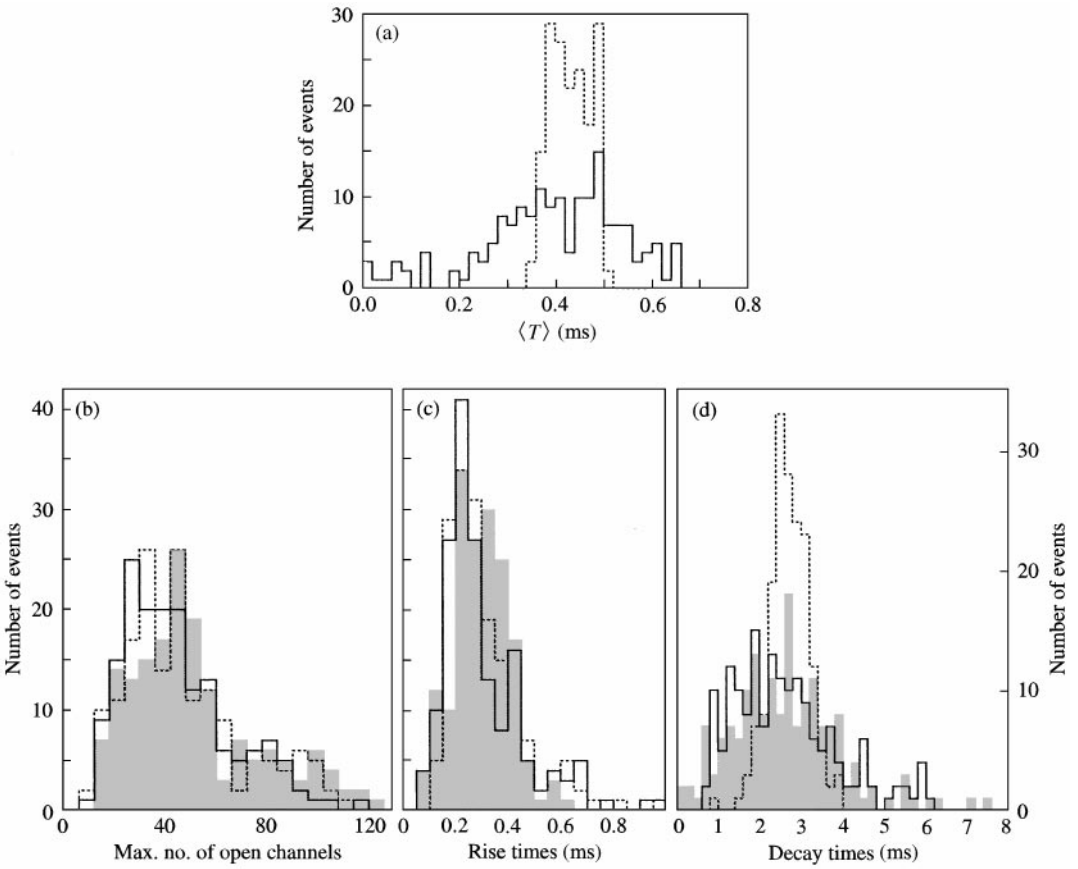

FIG. 8. Effect of fluctuations in the residence time $\langle T \rangle$ of transmitter (a) on the distribution of amplitudes (b), rise (c) and decay times (d); $\langle T \rangle = 0.43 \pm 0.04$ ms (white columns, ·····), $\langle T \rangle = 0.4 \pm 0.14$ ms (white columns, ——). Gray columns indicate the experimentally recorded miniature amplitudes. Monte Carlo simulations were run either for synaptic boutons with a fixed geometry (·····; absorbing boundary $r_{abs} = 500$ nm) or for varying geometries (——; absorbing boundaries (r_{abs} chosen randomly according to a truncated Gaussian distribution between 150 and 1000 nm, with $r_{abs} = 530 \pm 240$ nm), rest of parameters as in Fig. 5. In both cases 4000 transmitter molecules were released at each time randomly chosen release sites within the PSD of radius $r_{PSD} = 150$ nm.

variable receptor number [0.32 ± 0.18 ms, Fig. 5(b)] as compared to fixed vesicle content and fixed number (0.27 ± 0.1 ms, Fig. 6). We conclude that the distribution of rise times is largely controlled by the underlying receptor distribution and points towards homogeneous PSD shapes of approximately 150 nm radius at NTS neurons.

4.3. THE VARIABILITY OF mEPSC DECAY TIMES CAN BE EXPLAINED BY FLUCTUATIONS IN THE RESIDENCE TIME OF TRANSMITTER IN THE CLEFT

Monte Carlo simulations which are run for varying numbers of post-synaptic receptors (but for geometrically identical boutons) are able to reproduce the experimental distributions of amplitudes and rise times (see Fig. 5), but fail to account for the large range of variation observed in the distributions of decay times: while the experimentally observed decay times are strongly fluctuating (2.64 ± 1.30 ms, CV = 0.49), the Monte Carlo simulations are only able to resolve a small fraction of this variability (2.61 ± 0.48 ms, CV = 0.18). Furthermore, the spectrum of decay times (CV = 0.18, Fig. 5) as generated from Monte Carlo simulations with fluctuations in receptor number does not differ from the distribution of decay times for a fixed number of post-synaptic receptors (CV = 0.17, Fig. 6) and for additional variations in vesicle content (CV = 0.2, Fig. 6). As shown above, the

distribution of decay times is hardly changed by a varying PSD size—despite the large effect on the distribution of rise times. It should be noted that not only the mean value of τ_{decay}, but also its CV does not depend on the receptor distribution. Hence, the fact that mEPSCs are recorded from several synaptic boutons, which might exhibit a wide spectrum of PSD shapes (see e.g. Walmsley *et al*., 1998) and receptor numbers (see above), does not account for the broad fluctuations observed in the distribution of decay times.

It is possible that, due to individual morphological properties of single synaptic boutons, the time course of transmitter in the cleft is not the same for every synapse. We study the effect of fluctuations in the transmitter time course by varying the residence time of transmitter in the cleft $\langle T \rangle$ [eqn (4)]. Leaving the extension of the post-synaptic density fixed we modulate the residence time $\langle T \rangle$ by varying the absorbing boundary r_{abs} in our simulation model from run to run according to a Gaussian distribution with a mean of 530 nm and a standard deviation of 240 nm, considering only values of r_{abs} in between 150 and 1000 nm. This is thought to roughly represent heterogenities in the synaptic morphology as well as in the morphology of the extra-synaptic space. The chosen distribution of r_{abs} corresponds to fluctuations in the transmitter time course of $\langle T \rangle = 0.4 \pm 0.14$ ms. As displayed in Fig. 8 these fluctuations in residence time are able to produce the broad distribution of decay times (2.66 ± 1.32 ms, CV = 0.5) as observed in experiments. For comparison, we also show the distribution of decay times as calculated for weakly fluctuating residence times of $\langle T \rangle = 0.43 \pm 0.04$ ms, which cause a much sharper distribution of decay times (2.61 ± 0.48 ms, CV = 0.18) in disagreement with experiments. The distributions of maximum amplitudes (47.8 ± 23.2 channels vs. 45 ± 21.3 channels for fluctuating residence times) and rise times (0.32 ± 0.18 ms vs. 0.31 ± 0.17 ms for fluctuating residence times) remain approximately unaffected by strong fluctuations in transmitter time course. Hence, we conclude that the broad fluctuations in the decay times of EPSCs can be explained by variations in the time course of glutamate in the cleft, corresponding to a mean residence time of glutamate in the cleft of 0.4 ± 0.14 ms.

5. Discussion

Monte Carlo simulations have been used to study the origin of large fluctuations, which have been recorded in the time course of AMPA-mediated unitary EPSCs in brainstem interneurons. It has been shown that the release of a single vesicle activates about 70% of post-synaptic receptors. This leads to the conclusion that the large variability observed in the miniature amplitude distribution is due to fluctuations in the number of post-synaptic receptors. It is demonstrated that the distribution of decay times is not altered by fluctuations in receptor number, receptor arrangement or vesicle content, but reflects fluctuations in the residence time of the transmitter in the synaptic cleft. We conclude that most likely inhomogeneities in synaptic morphology, like morphological differences of extracellular space or inhomogeneous distributions of diffusion barriers in- and outside the cleft, are the reason for the fluctuations of the time course of transmitter in the cleft. The residence time of glutamate in the cleft at brainstem interneurons, which is able to account for the observed distribution of decay times, is estimated as 0.4 ± 0.13 ms. This is about half the estimate found at rat hippocampal neurons (Clements, 1996).

Our results differ from what has been expected by Faber *et al*. (1992), who suggested that due to a small number of post-synaptic receptors, the intrinsic noise of the receptor dynamics should provide the major contribution to synaptic variability. This assumption seems to hold for synaptic currents recorded at the mossy fiber synapse on CA3 pyramidal cells of rat hippocampus (Jonas *et al*., 1993), where it has been demonstrated that fluctuations in the time course of unitary EPSCs in reduced extracellular Ca^{2+} can be resolved by Monte Carlo simulations of a single synaptic bouton type [data taken from Trommershäuser *et al*. (1999) and displayed in Table 3]. This has led to the conclusion that for the latter type of synapses single-channel noise is the major source of synaptic variability.

However, the situation seems different at brainstem interneurons where single-channel noise fails to account for the whole spectrum of amplitudes and decay times (see Fig. 6). One

TABLE 3
Results for recorded and simulated EPSCs in CA3 pyramidal cells (Jonas et al., 1993; Trommershäuser et al., 1999)

	Maximum open probability	20–80% rise times	Decay times
Computer simulations	~ 63%	0.51 ± 0.26 ms	4.05 ± 1.15 ms
Experiments	~ 72%	0.5 ± 0.2 ms	4.1 ± 0.9 ms

possible source of synaptic variability is pointed out by e.g. Liu *et al.* (1999) or Min *et al.* (1998), who suggest that post-synaptic AMPA receptors in the hippocampus are not saturated leaving room for variations in the vesicle content contributing substantially to synaptic variability. This is not the situation at brainstem interneurons where we find that concentrations corresponding to the content of a single vesicle activate about 70% of the post-synaptic receptors. Several experiments on hippocampal and cerebellar synapses have led to the same conclusion (Hausser & Roth, 1997; Kullmann, 1993; Kullmann *et al.*, 1999; Jonas *et al.*, 1993; Marienhagen & Zippelius, 1995; Marienhagen *et al.*, 1997; Spruston *et al.*, 1995; Wahl *et al.*, 1996). The common idea is that an abundance of neurotransmitter remains in the cleft for approximately 1 ms (Barbour *et al.*, 1994; Clements, 1992; Spruston *et al.*, 1995; Clements, 1996) activating most of the post-synaptic receptors. If this scenario is true, variations in vesicle content should not create a large effect on the post-synaptic signal. As shown above this is confirmed by our Monte Carlo simulations, in which the vesicle content has been varied. We could not find any significant effect on the distributions of amplitudes, rise or decay times.

Several studies (see e.g. Edwards, 1995; Lim *et al.*, 1999; Oleskevich *et al.*, 1999; Peters & Kaiserman-Abramof, 1969; Walmsley *et al.*, 1998) have stressed that central synapses express a wide variety of PSD shapes and it has been assumed that the heterogeneity of the corresponding receptor distribution might contribute essentially to synaptic variability (Wahl *et al.*, 1996). Our simulations do not support this finding at NTS neurons. As demonstrated above the relatively narrow distribution of rise times is not consistent with a strong heterogeneity in PSD size. Hence, the latter has not been considered as a possible source for the broadening of the distribution of amplitudes and decay times.

Central synapses are not only thought to exhibit a heterogeneity in PSD shape, but also in synaptic morphology, which has an effect on the transmitter dynamics inside the cleft: it has been suggested that the spreading of neurotransmitter inside the cleft is affected by the tortuosity of the cleft (Garthwaite, 1985; Holmes, 1995; Ichimura & Hashimoto, 1988; Nicholson & Phillips, 1981; Rice *et al.*, 1985; Uteshev & Pennefather, 1997; Wahl *et al.*, 1996), by a dense staining, gel-like material (Edwards, 1995; Harris & Kater, 1994; Peters & Kaiserman-Abramof, 1969; Walmsley *et al.*, 1998; Van der Loos, 1963) or by interactions of the diffusing molecules with receptors, transporters or other binding sites (Rusakov & Kullmann, 1998; Trommershäuser *et al.*, 1999). Furthermore, it is likely that structural inhomogeneities in the vicinity of a synapse, for instance local narrowing of intracellular gaps, can significantly retard diffusion and act like a diffusion barrier (Barbour *et al.*, 1994; Kullmann *et al.*, 1999; Min *et al.*, 1998; Rossi *et al.*, 1995; Rusakov & Kullmann, 1998). Hence, fluctuations in the transmitter time course may arise from a heterogeneity of synaptic morphology or may be due to heterogeneity in distribution, number or efficiency of uptake molecules. However, bath application of the glutamate transporter blocker D-aspartate does not alter the EPSC kinetics. Control EPSCs do not differ from EPSCs recorded after inhibition of glutamate uptake with 1 mM D-aspartate (from Titz & Keller, 1997). We conclude that EPSCs at brainstem interneurons are not shaped by glutamate transporters and suggest that rather differences in synaptic morphology as well as inhomogeneous distributions of diffusion barriers in or outside

the cleft are responsible for fluctuations in the transmitter dynamics. Our simulations illustrate the effect of morphological heterogeneity on post-synaptic currents and demonstrate that the variability of decay times is resolved by fluctuations in the transmitter time course, which appears as a consequence of the geometrical heterogeneity. We can summarize that fluctuations in post-synaptic receptor number (77 ± 39 receptors per synapse) can account for the synaptic variability observed in amplitudes of miniature currents of brainstem interneurons, whereas the wide spectrum of decay times is explained by fluctuations in the transmitter time course (mean residence times of 0.4 ± 0.13 ms). We want to stress that synaptic mechanisms shaping the distributions of amplitudes are different from those affecting the distributions of rise and decay times. We therefore suggest that the analysis of miniature distributions and particularly of decay times can provide further insight into synaptic function.

We thank Bodo Vanselow for experimental help. This work has been supported by the DFG through Graduiertenkolleg *Organisation und Dynamik neuronaler Netzwerke*, by grant no. Ke 403/12-1, Ke 403/12-2, Zi 209/6-1 and Sonderforschungsbereich 406.

REFERENCES

AGMON, N. & EDELSTEIN, A. L. (1997). Collective binding properties of receptor arrays. *Biophys. J.* **72,** 1582–1594.

ATASSI, B. & GLAVINOVIC, M. I. (1999). Effect of cyclothiazide on spontaneous miniature excitatory postsynaptic currents in rat hippocampal pyramidal cells. *Pflügers Arch.* **437,** 471–478.

BARBOUR, B., KELLER, B. U., LLANO, I. & MARTY, A. (1994). Prolonged presence of glutamate during excitatory synaptic transmission to cerebellar Purkinje cells. *Neuron* **12,** 1331–1343.

BEKKERS, J. M. & STEVENS, C. F. (1995). Quantal analysis of EPSCs recorded from small numbers of synapses in hippocampal cultures. *J. Neurophysiol.* **73,** 1145–1156.

BEKKERS, J. M., RICHERSON, G. B. & STEVENS, C. F. (1990). Origin of variability in quantal size in cultured hippocampal neurons and hippocampal slices. *Proc. Natl Acad. Sci. U.S.A.* **87,** 5359–5362.

BENNETT, M. R., FARNELL, L., GIBSON, W. G. & LAVIDIS, N. A. (1997). Synaptic transmission at visualized sympathetic boutons: stochastic interaction between acetylcholine and its receptors. *Biophys. J.* **72,** 1595–1606.

BIER, M., KITS, K. S. & BORST, J. G. (1996). Relation between rise times and amplitudes of GABAergic postsynaptic currents. *J. Neurophysiol.* **75,** 1008–1012.

BORST, J. G. G., LODDER, J. C. & KITS, K. S. (1994). Large amplitude variability of GABAergic IPSCs in melano tropes from Xenopus leavis: evidence that quantal size differs between synapses. *J. Neurophysiol.* **71,** 639–655.

BRUNS, D. & JAHR, R. (1995). Real-time measurement of transmitter release from single synaptic vesicles. *Nature* **377,** 62–65.

CLEMENTS, J. D. (1996). Transmitter timecourse in the synaptic cleft: its role in central synaptic function. *Trends Neurosci.* **19,** 163–171.

CLEMENTS, J. D., LESTER, R. A. J., TONG, G., JAHR, C. E. & WESTBROOK, G. L. (1992). The time course of glutamate in the synaptic cleft. *Science* **258,** 1498–1501.

COLQUHOUN, D. & HAWKES, A. G. (1995). The principles of the stochastic interpretation of ion-channel mechanisms. In: *Single-Channel Recording* (Sakmann, B. & Neher, E., eds), 2nd edn., pp. 397–481. New York: Plenum Press.

DESTEXHE, A., MAINEN, Z. F. & SEJNOWSKI, T. J. (1994). Synthesis of models for excitable membranes, synaptic transmission and neuromodulation using a common kinetic formalism. *J. Comput. Neurosci.* **1,** 195–230.

DIAMOND, J. & JAHR, C. (1997). Transporters buffer synaptically released glutamate on a submillisecond time scale. *J. Neurosc.*, **17,** 4672–4687.

EDMONDS, B., GIBBS, A. J. & COLQUHOUN, D. (1995). Mechanisms of activation of glutamate receptors and the time course of excitatory synaptic currents. *Annu. Rev. Physiol.* **57,** 495–519.

EDWARDS, F. A. (1995). Anatomy and electrophysiology of fast central synapses lead to a structural model for long-term potentiation. *Physiol. Rev.* **75,** 759–787.

EDWARDS, F. A., KONNERTH, A. & SAKMANN, B. (1990). Quantal analysis of inhibitory synaptic transmission in the dentate gyrus of rat hippocampal slices: a patch clamp study. *J. Physiol.* (*Lond.*) **430,** 213–249.

FABER, D. S., YOUNG, W. S., LEGENDRE, P. & KORN, H. (1992). Intrinsic quantal variability due to stochastic properties of receptor-transmitter interactions. *Science* **258,** 1494–1498.

FORTI, L., BOSSI, M., BERGAMASCHI, A., VILLA, A. & MALGAROLI, A. (1997). Loose-patch recordings of single quanta at individual hippocampal synapses. *Nature* **388,** 874–878.

FRANKE, C., HATT, H. & DUDEL, J. (1987). Liquid filament switch off ultra-fast exchanges of solutions at excised patches of synaptic membrane of crayfish muscle. *Neurosci. Lett.* **77,** 199–204.

FRERKING, M. & WILSON, M. (1996). Saturation of postsynaptic receptors at central synapses? *Curr. Opin. Neurobiol.* **6,** 395–403.

FRERKING, M., BORGES, S. & WILSON, M. (1995). Variation in GABA mini amplitude is the consequence of variation in transmitter concentration. *Neuron* **15,** 885–895.

GARTHWAITE, J. (1985). Cellular uptake disguises action of L-glutamate on *N*-methyl-*D*-aspartate receptors. *Br. J. Pharmacol.* **85,** 297–307.

GLAVINOVIC, M. I. (1999). Monte Carlo simulation of vesicular release, spatiotemporal distribution of glutamate in synaptic cleft and generation of postsynaptic currents. *Pflügers Arch.* **437,** 462–470.

HAMILL, O. P., MARTY, A., NEHER, E., SAKMANN, B. & SIGWORTH, F. J. (1981). Improved patch-clamp techniques for high-resolution current recording from cells and cell-free membrane patches. *Pflügers Arch.* **391,** 85–100.

HARRIS, K. M. & KATER, S. B. (1994). Dendritic spines: cellular specializations imparting both stability and flexibility to synaptic function. *Annu. Rev. Neurosci.* **17,** 341–371.

HARRIS, K. M. & SULTAN, P. (1995). Variation in the number, location and size of synaptic vesicles provides an anatomical basis for the nonuniform probability of release at hippocampal CA1 synapses. *Neuropharmacology* **34,** 1387–1395.

HAUSSER, M. & ROTH, A. (1997). Dendritic and somatic glutamate receptor channels in rat cerebellar Purkinje cells. *J. Physiol.* (*Lond.*) **501,** 77–95.

HILLE, B. (1992). *Ionic Channels of Excitable Membranes*, 2nd edn. Sunderland: Sinauer Associates.

HOLMES, W. R. (1995). Modeling the effect of glutamate diffusion and uptake on NMDA and non-NMDA receptor saturation. *Biophys. J.* **69,** 1734–1747.

ICHIMURA, T. & HASHIMOTO, P. H. (1988). Structural components in the synaptic cleft captured by freeze-substitution and deep etching of directly frozen cerebellar cortex. *J. Neurocytol.* **17,** 3–12.

JAHN, K., BUFLER, J. & FRANKE, C. (1998). Kinetics of AMPA-type glutamate receptor channels in rat caudate-putamen neurones show a wide range of desensitization but distinct recovery characteristics. *Eur. J. Neurosci.* **10,** 664–672.

JONAS, P., MAJOR, G. & SAKMANN, B. (1993). Quantal components of unitary EPSCs at the mossy fiber synapse on CA3 pyramidal cells of rat hippocampus. *J. Physiol.* (*Lond.*) **472,** 615–663.

JONES, M. V. & WESTBROOK, G. L. (1996). The impact of receptor desensitization on fast synaptic transmission. *Trends Neurosci.* **19,** 96–101.

KLEINLE, J., VOGT, K., LUESCHER, H. R., MUELLER, L., SENN, W., WYLER, K. & STREIT, J. (1996). Transmitter concentration profiles in the synaptic cleft: analytical model of release and diffusion. *Biophys. J.* **71,** 2413–2426.

KULLMANN, D. M. (1993). Quantal variability of excitatory transmission in the hippocampus: implications for the opening probability of fast glutamate-gate channels. *Proc. R. Soc. Lond. B. Biol. Sci.* **22,** 107–116.

KULLMANN, D. M., MIN, M.-Y., ASZTELY, F. & RUSAKOV, D. (1999). Extracellular glutamate diffusion determines the occupancy of glutamate receptors at CA1 synapses in the hippocampus. *Phil. Trans. R. Soc. Lond. B* **354,** 395–402.

LIM, R., ALVAREZ, F. J. & WALMSLEY, B. (1999). Quantal size is correlated with receptor cluster area at glycinergic synapses in the rat brainstem. *J. Physiol.* (*Lond.*) **516,** 505–512.

LIU, G. & TSIEN, R. W. (1995). Properties of synaptic transmission at single hippocampal synaptic boutons. *Nature* **375,** 404–408.

LIU, G., CHOI, S. & TSIEN, R. W. (1999). Variability of neurotransmitter concentration and nonsaturation of postsynaptic AMPA receptors at synapses in hippocampal cultures and slices. *Neuron* **22,** 395–409.

LLANO, I., MARTY, A., ARMSTRONG, C. M. & KONNERTH, A. (1991). Synaptic- and agonist-induced excitatory currents of Purkinje cells in rat cerebellar slices. *J. Physiol. Lond.* **434,** 183–213.

MAINEN, Z. F., MALINOW, R. & SVOBODA, K. (1999). Synaptic calcium transients in single spines indicate that NMDA receptors are not saturated. *Nature* **399,** 151–155.

MARIENHAGEN, J. & ZIPPELIUS, A. (1995). Monte Carlo simulation of a structural model for long-term potentiation. *Super-computing in Brain Research*. (Hermann, H. J., Wolf, D. E. & Poeppel, E. eds). Singapore: World Scientific.

MARIENHAGEN, J., KELLER, B. U. & ZIPPELIUS, A. (1997). Kinetic model of excitatory synaptic transmission to cerebellar purkinje cells. *J. theor. Biol.* **188,** 227–240.

MIN, M.-Y., RUSAKOV, D. A. & KULLMANN, D. M. (1998). Activation of AMPA, kainate, and metabotropic receptors at hippocampal mossy fiber synapses: role of glutamate diffusion. *Neuron.* **21,** 561–570.

NICHOLSON, C. & PHILLIPS, J. M. (1981). Ion diffusion modified by tortuosity and volume fraction in the extracellular microenvironment of the rat cerebellum. *J. Physiol.* (*Lond.*) **321,** 225–257.

NUSSER, Z., CULL-CANDY, S. & FARRANT, M. (1997). Differences in synaptic $GABA_A$ receptor number underlie variation in GABA mini amplitude. *Neuron* **19,** 697–709.

OLESKEVICH, S., ALVAREZ, F. J. & WALMSLEY, B. (1999). Glycinergic miniature synaptic currents and receptor cluster sizes differ between spinal cord interneurons. *J. Neurophysiol.* **82,** 312–319.

PETERS, A. & KAISERMAN-ABRAMOF, I. R. (1969). The small pyramidal neuron of the rat cerebral cortex: the synapses upon dendritic spines. *Zeitsch. Zellforsch.* **100,** 487–506.

PRESS, W. P., TEUKOLSKY, S. A., VETTERING, W. T. & FLANNERY, B. P. (1992). *Numerical Recipes in C. The Art of Scientific Computing*, 2nd end. Cambridge: Cambridge University Press.

RICE, M. E., GERHARDT, G. A., HIERL, P. M., NAGY, G. & ADAMS, R. N. (1985). Diffusion coefficients of neurotransmitters and their metabolites in brain extracellular fluid space. *Neuroscience* **3,** 891–902.

ROSSI, D. J., ALFORD, S., MUGNAINI, E. & SLATER, N. T. (1995). Properties of transmission at a giant glutamatergic synapse in cerebellum: the mossy fiber-unipolar brush cell synapse. *J. Neurophysiol.* **74,** 24–42.

RUSAKOV, D. A. & KULLMANN, D. M. (1998). Geometric and viscous components of the tortuosity of the extracellular space in the brain. *Proc. Natl Acad. Sci. U.S.A.* **95,** 8975–8980.

SILVER, R. A., CULL-CANDY, S. G. & TAKAHASHI, T. (1996). Non-NMDA glutamate receptor occupancy and open probability at a rat cerebellar synapse with single and multiple release sites. *J. Physiol.* **494,** 231–250.

SIGWORTH, F. J. (1980). The variance of sodium current fluctuations at the node of Ranvier. *J. Physiol.* **307,** 97–129.

SPRUSTON, N., JONAS, P. & SAKMANN, B. (1995). Dendritic glutamate receptor channels in rat hippocampal CA3 and CA1 pyramidal neurons. *J. Physiol.* **482,** 325–352.

TANG, C. M., MARGULIS, M., SHI, Q. Y. & FIELDING, A. (1994). Saturation of postsynaptic glutamate receptors after quantal release of transmitter. *Neuron* **13,** 1385–1393.

TITZ, S. & KELLER, B. U. (1996). Functional diversity of excitatory synaptic currents mediated by long and short residence times of glutamate in the synaptic cleft. *Biophys. J.* **70,** A 372.

TITZ, S. & KELLER, B. U. (1997). Rapidly deactivating AMPA receptors determine excitatory synaptic transmission to interneurons in the nucleus tractus solitarius from rat. *J. Neurophysiol.* **78,** 82–91.

TONG, G. & JAHR, C. E. (1994). Block of glutamate transporters potentiates postsynaptic excitation. *Neuron* **13,** 1195–1203.

TROMMERSHÄUSER, J., MARIENHAGEN, J. & ZIPPELIUS, A. (1999). Stochastic model of central synapses: slow diffusion

of transmitter interacting with spatially distributed receptors and transporters. *J. theor. Biol.* **198,** 101–120.

UTESHEV, V. V. & PENNEFATHER, P. S. (1996). A mathematical description of MPSC generation at CNS synapses. *Biophys. J.* **71,** 1256–1266.

UTESHEV, V. V. & PENNEFATHER, P. S. (1997). Analytical description of the activation of multi-state receptors by continuous neurotransmitter signals at brain synapses. *Biophys. J.* **72,** 1127–1134.

VAN DEN LOOS, H. (1963). Fine structure of synapses in the cerebral cortex. *Zeitsch. Zellforsch.* **60,** 815–825.

WAHL, L. M., POUZAT, C. & STRATFORD, K. J. (1996). Monte Carlo simulation of fast excitatory synaptic transmission at a hippocampal synapse. *J. Neurophysiol.* **75,** 597–608.

WALMSLEY, B., ALVAREZ, F. J. & FYFFE, R. E. W. (1998). Diversity of structure and function at mammalian central synapses. *Trends Neurosci.* **21,** 81–88.